Improved Image Denoising with Adaptive Nonlocal Means (ANL-Means) Algorithm

Tanaphol Thaipanich, Byung Tae Oh, Ping-Hao Wu, Daru Xu and C.-C. Jay Kuo, *Fellow*, IEEE

**Abstract — ***An adaptive nonlocal-means (ANL-means) algorithm for image denoising is proposed in this work. It employs the singular value decomposition (SVD) method and the K-means clustering (K-means) technique to achieve robust block classification in noisy images. Then, a local window is adaptively adjusted to match the local property of a block and a rotated matching algorithm that aligns the dominant orientation of a local region is adopted for similarity matching. Furthermore, the noise level is estimated using the block classification result and the Laplacian operator. Experimental results are given to demonstrate the superior denoising performance of the proposed ANL-means denoising technique over various image denoising benchmarks in terms of the PSNR value and perceptual quality comparison, where images corrupted by additive white Gaussian noise (AWGN) are tested.*

Index Terms — Nonlocal means, NL-means, Adaptive nonlocal-means, ANL-means, Image denoising, AWGN.

I. INTRODUCTION

Image denoising [1], [2] is one of the classical problems in digital image processing, and has been studied for nearly half a century due to its important role as a pre-processing step in various electronic imaging applications. Its objective is to recover the best estimate of the original image from its noisy version. Several denoising methods have been proposed such as neighborhood filtering [3], median filtering [4], [5], total variation minimization [6], [7], Wiener filtering [8], wavelet filtering [9], [10], [11], [12] Gaussian scalar mixture [13], methods based on partial differential equation solution [14], etc.

Early denoising techniques such as the Gaussian and the mean filtering are suitable for smooth regions but they yield blurred edge and texture regions. Unlike the aforementioned techniques, the Wiener filtering method operates in the frequency domain. The denoised image is estimated by the inverse transform of the filtered coefficients, which results in an improved edge region.

This paper was presented in part at The International Conference on Consumer Electronics 2010 (ICCE2010), Las Vegas, NV, USA

Tanaphol Thaipanich, Byung Tae Oh, Ping-hao Wu, Daru Xu and C.-C. Jay Kuo are with the Ming Hsieh Department of Electrical Engineering, University of Southern California, Los Angeles, CA 90089, USA (E-mails: tthaipanich@push.co.th, btoh77@gmail.com, pinhoramic@gmail.com, daruxu@usc.edu and cckuo@sipi.usc.edu)

This research is supported in part by a gift grant from Xerox.

For the total variation minimization technique, the total variation of an image is minimized subject to a constraint derived from noise characteristics. This technique can effectively preserve straight edges. However, if the Lagrange multiplier is too small, fine details could be over-smoothed. On the other hand, the flat region of the denoised image may suffer from the mask effect if the Lagrange multiplier is too large. The selection of a proper value of the Lagrange multiplier is not trivial.

The nonlocal means (NL-means) algorithm [15], [16], [17] has offered remarkably promising results. Unlike previous denoising methods which were developed under the local regularity assumption, the NL-means exploits the spatial correlation in the entire image for noise removal. It adjusts each pixel value with a weighted average of other pixels whose neighborhood has a similar geometrical configuration. Since image pixels are highly correlated while noise is typically independently and identically distributed (i.i.d.), averaging of these pixels results in noise cancellation and yields a pixel that is similar to its original value. Several papers have been published on the speed-up of the NL-means algorithms [18], [19], [20], [21].

In this research, we propose an adaptive NL-means (ANL-means) algorithm [22], [23], [24] that improves the similarity matching process and denoising parameters based on the local structure of a pixel. The singular value decomposition (SVD) method and the K-means clustering (K-means) technique are employed for robust block classification in noisy images. The similarity matching process is enhanced by allowing more candidates through rotated matching via dominant orientation alignment. Moreover, a scheme to estimate the noise level based on the Laplacian operator [19] is presented. It is shown by experimental results that the ANL-means algorithm outperforms the traditional NL-means algorithm significantly for a wide range of test images and conditions. The ANL-means algorithm is especially advantageous when the noise level is high.

The rest of this paper is organized as follows. The new ANL-means algorithm is proposed in Sec. II. The noise level estimation scheme for AWGN is presented in Sec. III. Experimental results of the ANL-means algorithm under various conditions are shown in Sec. IV. Finally, concluding remarks are given in Sec. V.

Manuscript received 10/06/10
Current version published 12/23/10
Electronic version published 12/30/10.

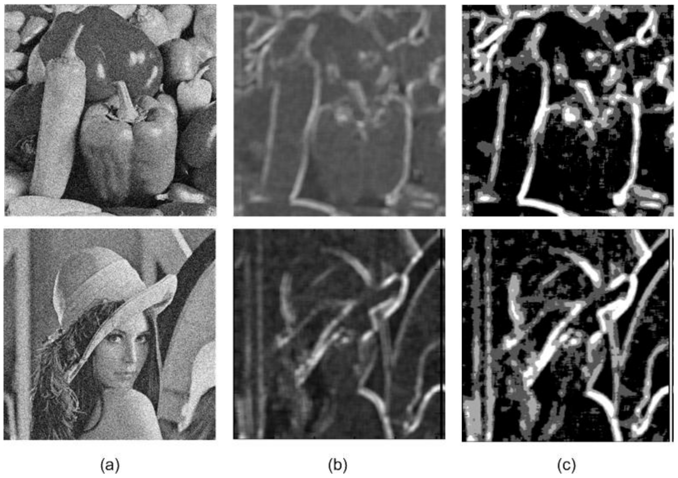

Fig. 1. Examples of block classification via SVD and K-means: (a) noisy image, (b) energy in the dominant direction - the brighter region has a more dominant edge direction and (c) classification results with the K-means algorithm, where different gray values correspond to different classes.

II. Adaptive Nonlocal Means (ANL-Means) Algorithm

The basic NL algorithm [15] is described below. For given noisy image $f = \{f(i) \mid i \in \Omega\}$, the denoised value $\hat{f}(i)$ at pixel i is obtained by a weighted average of all pixels in its neighborhood Ω_S:

$$\hat{f}(i) = \frac{1}{C(i)} \sum_{j \in \Omega_S} w(i,j) f(j), \tag{1}$$

where

$$C(i) = \sum_{j \in \Omega_S} w(i,j) \tag{2}$$

is a normalization constant and weight $w(i,j)$ is determined by the similarity of the Gaussian neighborhood between pixels i and j, which can be expressed as

$$w(i,j) = \exp\left(-\frac{\|N_i - N_j\|_{2,a}^2}{h^2}\right), \tag{3}$$

and where N_i denotes a square neighborhood centered at pixel i, $\|\cdot\|_{2,a}$ is a Gaussian weighted Euclidean distance function, a is the standard deviation of the Gaussian kernel, and h is the decay parameter.

The proposed adaptive technique has three unique features:

1) employing the singular value decomposition (SVD) method and k-means clustering (K-means) technique for robust block classification;

2) adjusting the local window adaptively to match the local property of a block; and

3) applying a rotated matching algorithm for better similarity matching.

Feature 1 will be described in Sec. II-A while Features 2 and 3 will be detailed in Sec. II-B.

A. Block Classification

Adaptation of the NL-means algorithm is achieved based on the block classification result. In this work, block classification is achieved by applying the SVD to the gradient field of each block [9]. For a smooth region, there is no dominant direction and all computed singular values are small. For an oriented edge/texture region, there is a dominant direction and the corresponding singular value is significantly larger than others.

Specifically, we can express the above idea in terms of mathematical equations as follows. For a spatial block of size $n \times n = N$, we can group its gradient values into matrix G of size $N \times 2$ and compute its SVD via

$$G = \left[\nabla f(1)^T \ \nabla f(2)^T \cdots \nabla f(N)^T\right]^T \ and \ G = USV^T \tag{4}$$

where

$$\nabla f(i) = \left[\frac{\partial f(i)}{\partial x} \quad \frac{\partial f(i)}{\partial y}\right]^T \tag{5}$$

is the gradient of image f at point i, U is an N-by-N orthogonal matrix, S is an N-by-2 matrix that contains singular values and V is a 2-by-2 orthogonal matrix which gives the dominant orientation of the gradient field. Since the white noise does not have any preferred direction, we can classify each block effectively based on the magnitude of the singular value in the dominant direction. In order to perform adaptive classification, we employ the K-means clustering technique. Let $s(i)$ be the singular value in the dominant direction of the block centered at pixel i. The K-means algorithm partitions into K classes $C = \{c_1, c_2, \ldots, c_k\}$ while minimizing the within-cluster sum of squares as

$$\arg\min_C \sum_{k=1}^{K} \sum_{s(i) \in c_k} |s(i) - \mu_k|^2, \tag{6}$$

where μ_k is the mean of c_k. An example of energy in the dominant direction and the corresponding classification result is presented in Figs. 1-b and 1-c, respectively.

B. Adaptive Window Adjustment and Rotated Matching

To exploit the local property and reduce noise in different regions, we adaptively choose the matching window size based on the classification result. For the edge/texture region, we employ a small matching window. In contrast, a larger matching window is adopted for the smooth region. In practice, we use a small window (7×7) in the strong edge/texture region, a large window (19×19) in the smooth region, and a medium window (13×13) in other regions.

Furthermore, we employ a rotated matching process that allows more candidates of similar image blocks. The matching kernel of the conventional NL-means algorithm is the Gaussian weighted Euclidean distance function, which only recognizes similar blocks of displacement. This matching kernel cannot select a distant region that is similar but with an orientation angle since the distance value can be large. As a result, the conventional scheme cannot fully exploit the self-similarity existing in regions such as the object contour.

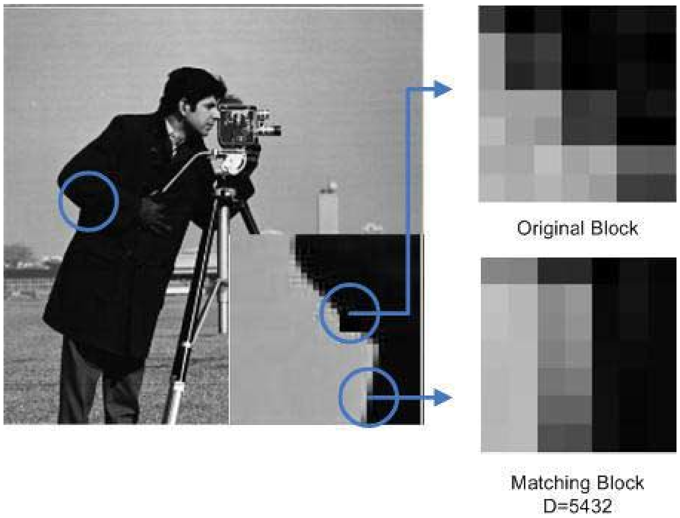

Figure 2: Example of large similarity distance between two neighboring blocks that contain the same object contour.

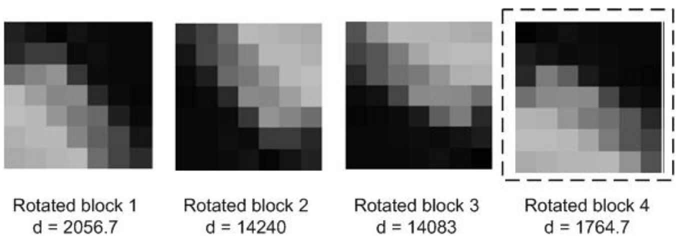

Figure 3: Four rotated matching blocks with dominant orientations equal to θ, $\theta+180$, $-\theta$ and $-\theta+180$ degrees.

ANL-means algorithm can effectively identify block with shifted orientation as a close match. In general, the candidate block can be rotated in various orientations until the lowest similarity distance is acquired. To speed up the matching process, we consider only a set of rotated blocks that have their dominant orientation aligned well with that of the target block. To be more specific, let $v_1 = [\upsilon_1\ \upsilon_2]^T$ be the first column of V in Eq. (4). We can obtain the dominant orientation of the gradient field of a given block by calculating

$$\theta = \arctan(\frac{\upsilon_1}{\upsilon_2}) . \tag{7}$$

Since gradient field doesn't have direction, we need to create four rotated blocks with dominant orientations equal to θ, $\theta+180$, $-\theta$ and $-\theta+180$ degrees in order to align the dominant orientation of matching block with that of original block. The best angle could be further selected based on simple examination of local gradient distribution and average values on both sides across the edge. Block rotation is achieved by bicubic interpolation and reflection operation. Since the block rotation process takes a higher computational complexity, we apply this technique only to blocks that have a strong dominant orientation. Fig. 2 illustrates the large Gaussian weighted Euclidean distance (Distance = 5432) between the original block and the matching candidate which are derived from the same object contour. The large similarity distance is caused by rotated block transformation. The example of four rotated matching candidates is shown in Fig. 3. In this instance, the rotated block no. 4 is determined as a close match to original block (Distance = 1764).

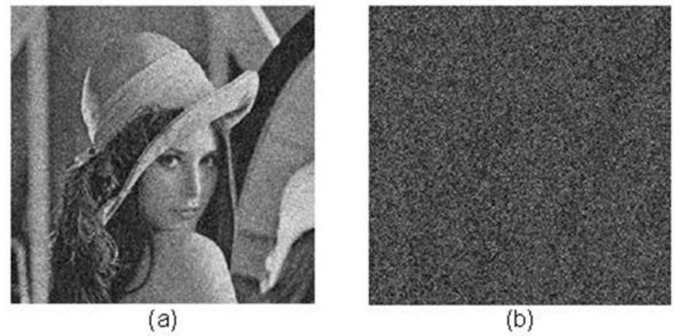

Figure 4: Illustration of the noise level estimation scheme using the Laplacian operator: (a) noisy Lena image with AWGN (σ_n = 40) and (b) the processed image using the Laplacian operator.

III. Noise Level Estimation

Accurate estimation of the noise level is critical to the performance of the NL-means algorithm since the weight decay factor is determined by the estimated noise level [25], [26], [27]. An under-estimation of the standard deviation of noise σ_n would lower the denoising performance of the NL-means and yields a noisy result. On the other hand, an over-estimation of the noise parameter would result in a burring denoised image. In this section, we propose a low complexity method to estimate the variance of the Gaussian noise from a noisy image based on the Laplacian operator and classification results from the ANL-means algorithm. A noise variance estimation technique was proposed in [28], which uses the Laplacian operator to suppress the image structure as illustrated in Fig. 4. The variance of the output image provides an estimation of the noise variance. We express the discrete Laplacian operator by

$$M = \begin{bmatrix} 1 & -2 & 1 \\ -2 & 4 & -2 \\ 1 & -2 & 1 \end{bmatrix} \tag{8}$$

Then, the application of the Laplacian operator M to image I at position (x, y) can be written as $I(x, y) * M$. If noise at a pixel has standard deviation σ_n, then $I(x, y) * M$ has zero mean and variance of $36\sigma_n^2$. The variance of noise in I can be computed as

$$\sigma_n^2 = \frac{1}{36 \times W \times H} \sum_{\forall x,y} (I(x, y) * M)^2, \tag{9}$$

where W and H are the image width and the image height, respectively. However, since strong edges and complex textures can over-estimate the noise variance [23], we use the block classification method proposed in Sec. II-A to locate the smooth region for accurate variance estimation. This can be written as

Table 1: Performance comparison of noise level estimation schemes using the Laplacian operator and the proposed technique for AWGN of three variance levels (σ_n = 20, 30 and 40)

Image	Noise parameter											
	σ = 20				σ = 30				σ = 40			
	Laplacian		Proposed		Laplacian		Proposed		Laplacian		Proposed	
	Est.	Δ	Est.	Δ	Est.	Δ	Est.	Δ	Est.	Δ	Est.	Δ
Lena	20.03	0.03	20.10	0.10	29.47	0.53	29.60	0.40	38.46	1.54	38.59	1.41
Zelda	19.56	0.44	20.03	0.03	28.63	1.37	29.56	0.44	37.11	2.89	38.47	1.53
Peppers	20.44	0.44	20.70	0.70	29.68	0.32	30.11	0.11	38.47	1.53	39.13	0.87
Fruits	19.85	0.15	20.05	0.05	29.15	0.85	29.68	0.32	38.06	1.94	38.82	1.18
Cameraman	19.18	0.82	19.99	0.01	28.20	1.80	29.69	0.31	37.09	2.91	39.20	0.80
Elaine	21.02	1.02	21.14	1.14	30.37	0.37	30.57	0.57	39.31	0.69	39.59	0.41
Girlface	18.85	1.15	20.09	0.09	27.54	2.46	29.54	0.46	35.82	4.18	38.44	1.56
Summary		**0.58**		**0.30**		**1.10**		**0.37**		**2.24**		**1.11**

Table 2: The PSNR comparison between the NL-means and the ANL-means algorithms for the AWGN of three standard deviation values (σ_n = 20, 30 and 40).

Image	Average PSNR (dB)								
	Sigma = 20			Sigma = 30			Sigma = 40		
	NL	ANL	Δ	NL	ANL	Δ	NL	ANL	Δ
Lena	31.02	31.98	0.96	27.50	30.04	2.54	24.37	28.27	3.90
Zelda	31.85	32.83	0.98	28.18	30.72	2.55	25.06	28.76	3.70
Peppers	30.93	31.59	0.65	27.50	29.79	2.29	24.40	28.00	3.60
Airplain	30.52	30.93	0.41	27.20	29.05	1.85	24.34	27.41	3.07
Barbara	29.85	30.30	0.45	26.65	28.41	1.76	23.89	26.74	2.85
Elaine	30.40	30.82	0.42	27.30	29.58	2.28	24.32	28.10	3.78
Girlface	31.75	32.29	0.54	28.12	29.98	1.86	25.06	27.92	2.86
Average	**30.90**	**31.53**	**0.63**	**27.49**	**29.65**	**2.16**	**24.49**	**27.89**	**3.39**

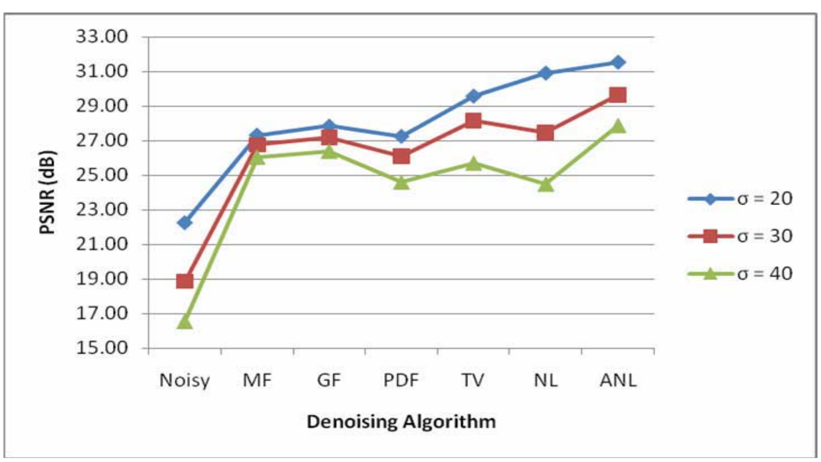

Figure 5: Comparison of the averaged PSNR values of six denoising algorithms applied to seven test images corrupted by the AWGN with three standard deviation values (σ_n = 20, 30 and 40).

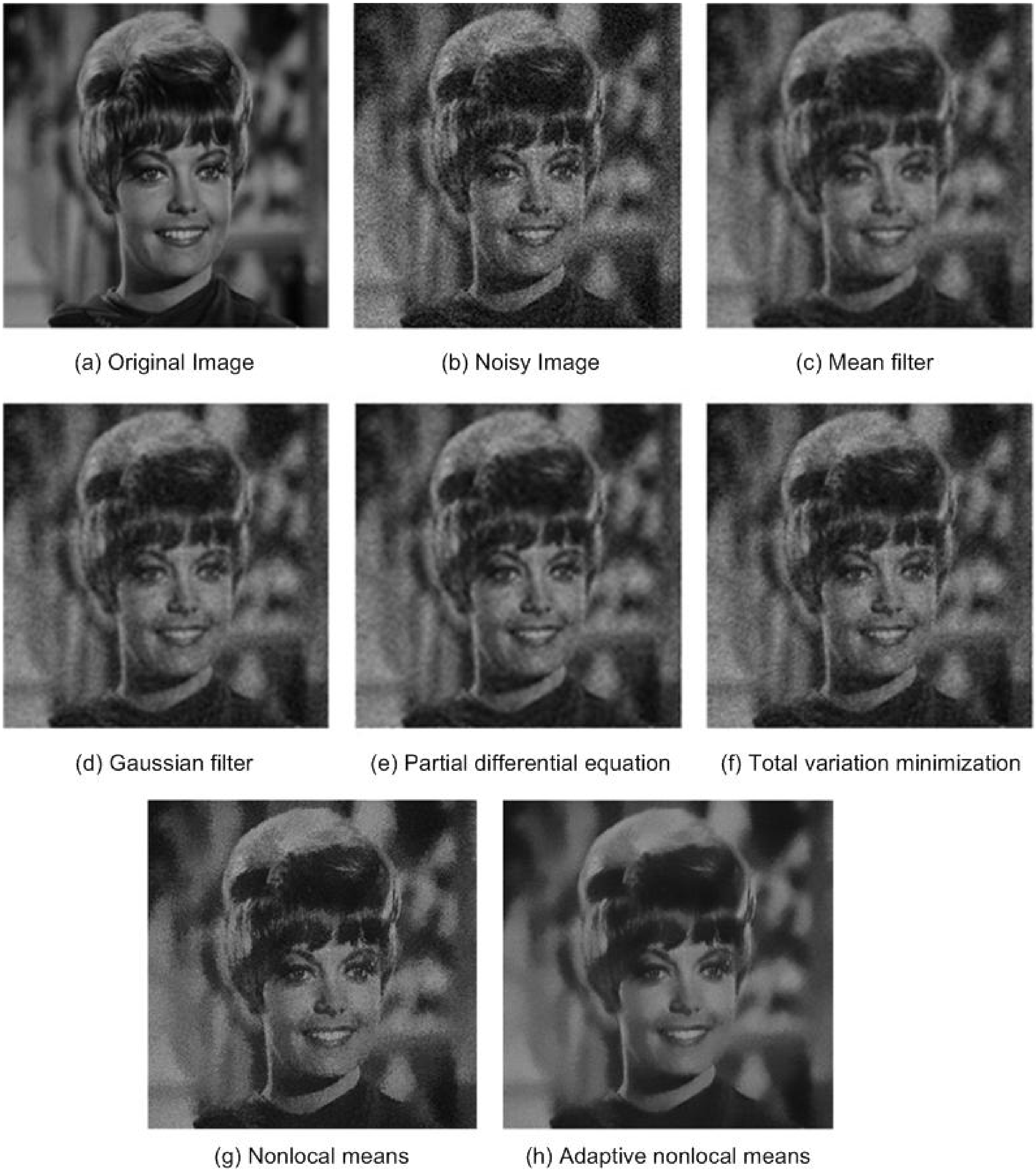

Figure 6: Visual quality comparison of various denoising algorithms for image Zelda corrupted by AWGN with σ_n = 40.

(a) Original Image (b) Noisy Image (c) Mean filter

(d) Gaussian filter (e) Partial differential equation (f) Total variation minimization

(g) Nonlocal means (h) Adaptive nonlocal means

Figure 7: Visual quality comparison of various denoising algorithms for image Lena corrupted by AWGN with σ_n = 40.

Table 3: The simulation time comparison between the NL-means and the ANL-means algorithms for image Lena corrupted by AWGN (σ_n = 20, 40).

σ	NL	ANL w/o rotation	ANL with rotation (1 angle)	ANL with rotation (4 angles)
20	12 sec	40 sec	43 sec	51 sec
40	12 sec	36 sec	41 sec	50 sec

$$\sigma_n^2 = \frac{1}{36 \times N_s} \sum_{\forall x,y \in \Omega_s} (I(x,y) * M)^2, \qquad (10)$$

where N_s is the total number of classified pixels in the smooth region denoted by Ω_s.

We compare the performance of the noise level estimation using the Laplacian operator and the proposed scheme in Table 1. In this experiment, seven test images are corrupted by AWGN with zero mean and standard deviation σ_n = 30, 40 and 50. We see that the proposed technique is effective and robust in all noise levels. On the average, the proposed scheme has an estimated variance error of 0.30, 0.37 and 1.11 while the Laplacian technique has an estimated error of 0.58, 1.10 and 2.24 for σ_n = 20, 30 and 40, respectively.

IV. Experimental Results

In this section, the denoising performance of the proposed ANL-means algorithm is compared with five well known denoising algorithms: 1) the mean filter (MF), 2) the Gaussian filtering (GF), 3) the method based the partial differential equation (PDE) [14], 4) the total variation (TV) minimization [6], and 5) the traditional NL-means algorithm [15].

First, we consider a set of seven representative test images corrupted by the zero-mean AWGN with standard deviation σ_n = 20, 30 and 40. For each case, three Gaussian noise patterns are generated and the averaged PSNR results of these three denoised images are reported. The PSNR comparison between the NL-means and the ANL-means algorithms for each test image of different standard deviation values are listed in Table 2. The averaged PSNR performance of six denoising algorithms is compared in Fig. 5. We see that ANL-means has a substantial PSNR gain over other denoising benchmarks. The average PSNR of the ANL-means scheme is approximately 2.98, 2.55, 3.70, 1.88 and 2.06 dB better than MF, GF, PDE, TV and NL-means, respectively. The ANL-means achieves an average PSNR improvement of 0.63, 2.16 and 3.39 dB over the NL-means for σ_n = 20, 30 and 40, respectively.

The denoised images obtained with various algorithms are shown in Figs. 6 and 7 for visual comparison. The denoising results using MF, GF and PDE might have higher PSNR yet the visual quality is actually poorer due to blurred edges. On the other hand, the TV and the NL-means denoising algorithms preserve sharp edges and object contours reasonably well. We see that the proposed ANL-means scheme provides much better visual quality, where noise is strongly suppressed in the smooth region while sharp edges around the object contour are well preserved.

The higher quality of the proposed ANL-means scheme is achieved at the cost of higher complexity. To measure this complexity increase quantitatively, we compare the computational time required by the NL-means and the proposed ANL-means algorithms in Table 3. The experiments were performed on a dual-core computer with multi-threading programming. We see that the computational time of the ANL-means algorithm is higher than that of the NL-means by a factor of 3 or 4. This is most attributed by larger matching windows which were adopted adaptively. The complexity required by the block rotation operation can be effectively reduced by the angle selection scheme, as there is no need to perform rotation with 4 candidate angles but only one suitable angle.

V. Conclusion

An adaptive NL-means scheme was proposed in this work, which was shown to be effective in the denoising of highly noisy images corrupted by AWGN noise. The proposed ANL-means can classify noisy image effectively via SVD and K-means clustering technique. The block classification results are utilized to adjust the similarity measure window size adaptively. Furthermore, a rotated block matching algorithm is employed to enhance the similarity matching process. The noise level can be estimated more accurately using a modified Laplacian noise estimation method. It was shown by experimental results that the performance of the proposed ANL-means scheme outperforms several well-known denoising benchmarks in terms of the PSNR value and visual quality.

Acknowledgment

This research is supported in part by a gift grant from Xerox

References

[1] A. Buades, B. Coll, and J. M. Morel, “A review of image denoising algorithms, with a new one,” Multiscale Modeling and Simulation, vol. 4, no. 2, pp. 490–530, 2005.

[2] M. C. Motwani, M. C. Gadiya, C. Rakhi, R. C. Motwani, and F. C. Harris, “Survey of image denoising techniques,” Proc. of GSPx, Santa Clara, CA, USA, 2004.

[3] M. Lindenbaum, M. Fischer, and A. M. Bruckstein, “On Gabor's contribution to image-enhancement,” Pattern Recognition, vol. 27, pp.1-8, 1994.

[4] H. Ibrahim, N.S.P. Kong, and T. F. Ng, “Simple adaptive median filter for the removal of impulse noise from highly corrupted images,” IEEE Trans. on Consumer Electronics, Vol. 54, No. 4, pp. 1920 - 1927, 2005.

[5] L. Wenbin, “Efficient removal of impulse noise from digital images,” IEEE Trans. on Consumer Electronics, Vol. 52, No. 2, pp. 523 - 527, 2006.

[6] A. Chambolle, “An algorithm for total variation minimization and applications,” Journal of Mathmatical Imaging and Vision 20 (1-2): 89-97, 2004.

[7] L. Rudin, S. Osher, and E. Fatemi, “Nonlinear total variation based noise removal algorithms,” Physica D, 60: pp. 259–268, 1992.

[8] S. Ghael, A. M. Sayeed, and R. G. Baraniuk, “Improved wavelet denoising via empirical Wiener filtering,” Proc. SPIE, Wavelet Applications in Signal and Image Processing V, vol. 3169, pp. 389–399, Oct 1997.

[9] D. L. Donoho, “De-noising by soft-thresholding”, IEEE Trans. on Information Theory, vol.41, no.3, pp.613-627, May1995.

[10] I. K. Fodor and C. Kamath, “Denoising through wavelet shrinkage: An empirical study”, Center for applied science computing Lawrence Livermore National Laboratory, July 27, 2001.

[11] J. Romberg, H. Choi, and R. G. Baraniuk, “Bayesian wavelet domain image modeling using hidden Markov models,” IEEE Trans. on Image Processing, vol. 10, pp. 1056-1068, July 2001.

[12] J. Kim, “Adaptive blocking artifact reduction using wavelet-based block analysis,” IEEE Trans. on Consumer Electronics, Vol. 55, No. 2, pp. 933 - 940, 2008.

[13] J. Portilla, V. Strela, M. J. Wainwright, and E. P. Simoncelli, “Image denoising using scale mixtures of Gaussians in the wavelet domain,” IEEE Trans. on Image Processing, vol. 12, no. 11, pp. 1338–1351, 2003.

[14] M. Lysaker, A. Lundervold, and X.-C. Taj, “Noise removal using fourth-order partial differential equations with applications to medical magnetic resonance images in space and time,” IEEE Trans. on Image Processing, vol. 12, pp. 1579–1590, 2003.

[15] A. Buades, B. Coll, and J. M. Morel, “A non local algorithm for image denoising,” IEEE Conf. on Computer Vision and Pattern Recognition (CVPR), vol. 2, 2005, pp. 60–65.

[16] P. Chatterjee and P. Milanfar, “A generalization of non-local means via kernel regression,” Proc. SPIE Conf. on Computational Imaging, San Jose, January 2008.

[17] J. Dinesh Peter, V. K. Govindan, and A. T. Mathew, “Robust estimation approach for nonlocal-means denoising based on structurally similar patches,” Int. J. Open Problems Compt. Math., vol. 2, no. 2, June 2009.

[18] Y. L. Liu, J. Wang, X. Chen, Y. W. Guo, and Q. S. Peng, “A robust and fast non-local means algorithm for image denoising,” Journal of Computer Science and Technology, Vol. 23, No. 2, pp. 270-279, 2008.

[19] S. C. Tai and S. M. Yang, “A fast method for image noise estimation using Laplacian operator and adaptive edge detection,” 3rd Int. Symposium on Communications, Control and Signal Processing, 2008 (ISCCSP 2008), pp. 1077-1081, Mar 2008.

[20] R. Vignesh, B. T. Oh, and C.-C. J. Kuo, “Fast non-local means (NLM) computation with probabilistic early termination,” IEEE Signal Processing Letters, Vol. 17, No. 3, pp. 277-280, March 2010.

[21] J. Wang, Y. Guo, Y. Ying, Y. Liu, and Q. Peng, “Fast non-local algorithm for image denoising”, IEEE Int. Conf. on Image Processing, pp. 1429-1432, 2006.

[22] C. Kervrann and J. Boulanger, “Optimal spatial adaptation for patch-based image denoising,” IEEE Trans. on Image Processing, Vol. 15, No. 10, pp. 2866-2878, 2006.

[23] T. Thaipanich and C.-C. J. Kuo, “An adaptive nonlocal means scheme for medical image denoising,” SPIE Medical Imaging, San Diego, CA, USA, February 2010.

[24] T. Thaipanich, B. T. Oh, P.-H. Wu, and C.-C. J. Kuo, “Adaptive nonlocal means algorithm for image denoising,” IEEE Int. Conf. on Consumer Electronics, Las, Vegas, NV, USA, January 2010.

[25] D. H. Shin, R. H. Park, S. Yang, and J. H. Jung, “Block-based noise estimation using adaptive Gaussian filtering,” IEEE Trans. on Consumer Electronics, Vol. 51, No. 1, pp. 218 – 226, 2005.

[26] A. Bosco, A. Bruna, G. Messina, and G. Spampinato, “Fast method for noise level estimation and integrated noise reduction,” IEEE Trans. on Consumer Electronics, Vol. 51 , No. 3, pp. 1028 – 1033, 2005.

[27] S. W. Lee, V. Maik, J. Jang, J. Shin, and J. Paik, “Noise-adaptive spatio-temporal filter for real-time noise removal in low light level images,” IEEE Trans. on Consumer Electronics, Vol. 51, No. 2, pp. 648 - 653, 2005.

[28] J. Immerkær, “Fast noise variance estimation,” Computer Vision and Image Understanding, Vol. 64, No. 2, pp. 300-302, Sep. 1996.

BIOGRAPHIES

Tanaphol Thaipanich received his B.Eng degree in Electrical Engineering at Chulalongkorn University, Bangkok, Thailand in 2002, and his M.S. and Ph.D. degree in Electrical Engineering at the University of Southern California (USC), Los Angeles, CA, USA in 2009. His research interests include computer vision, video error concealment, video frame rate up-conversion and image denoising.

Byung Tae Oh Byung Tae Oh received his B.S. degree in Electrical Engineering at Yonsei University, Seoul, Korea, in 2003, and his M.S. and Ph.D. degree in Electrical Engineering at the University of Southern California (USC), LA, CA in 2007 and 2009, respectively. His research interests include image and video restoration, super-resolution, texture analysis/synthesis and video pre/post-processing for efficient coding.

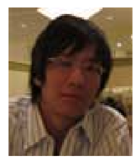

Ping-Hao Wu is a Ph.D. student in the Ming Hsieh Department of Electrical Engineering at the University of Southern California (USC). He received his B.S. degree in Electrical Engineering and the M.S. degree in Communication Engineering from the National Taiwan University in 2004 and 2006, respectively. His research interests include digital signal processing, video genre classification, video database management and image/video processing.

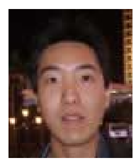

Daru Xu is a Master student in the Ming Hsieh Department of Electrical Engineering at the University of Southern California (USC). He received his B.S. degree in Electrical Engineering from the Shenzhen University in 2007. His research interests include digital signal processing, machine learning, multi-threading and image/video processing.

C.-C. Jay Kuo received the B.S. degree from the National Taiwan University, Taipei, in 1980 and the M.S. and Ph.D. degrees from the Massachusetts Institute of Technology, Cambridge, in 1985 and 1987, respectively, all in Electrical Engineering. He is Director of the Signal and Image Processing Institute (SIPI) and Professor of Electrical Engineering, Computer Science and Mathematics at the University of Southern California (USC). His research interests are in the areas of digital image/video analysis and modeling, multimedia data compression, communication and networking and multimedia database management. Dr. Kuo has guided 105 students to their Ph.D. degrees and supervised 20 postdoctoral research fellows. He is a co-author of about 180 journal papers, 800 conference papers and 10 books. Dr. Kuo is a Fellow of IEEE and SPIE. He is Editor-in-Chief for the Journal of Visual Communication and Image Representation, and Editor for the Journal of Information Science and Engineering, LNCS Transactions on Data Hiding and Multimedia Security and the EURASIP Journal of Applied Signal Processing. Dr. Kuo received the National Science Foundation Young Investigator Award (NYI) and Presidential Faculty Fellow (PFF) Award in 1992 and 1993, respectively. He was an IEEE Signal Processing Society Distinguished Lecturer in 2006, the recipient of the Electronic Imaging Scientist of the Year Award in 2010 and the holder of the 2010-2011 Fulbright-Nokia Distinguished Chair in Information and Communications Technologies.